Scaling SDM Optical Networks Using Full-Spectrum Spatial Switching

Alaelson C. Jatoba-Neto, Darli A. A. Mello, Christian E. Rothenberg, Sercan Ö. Arik, and Joseph M. Kahn

***Abstract*—In today's optical networks, the capacity supported by a single optical fiber is far higher than the demand between source–destination pairs. Thus, to take advantage of the installed capacity, lightpaths allocated between distinct source–destination pairs share the capacity provided by an optical fiber. This sharing is only possible if these lightpaths have different wavelengths. With the exponential evolution of traffic, the demand between source–destination pairs in a network can approach or exceed the capacity of a single fiber. In this scenario, space-division multiplexing (SDM) networks appear as a viable option, and new network-sharing technologies become relevant. In this paper, we study different switching approaches for SDM networks with uncoupled spatial superchannels—such as networks with multicore fibers or bundles of single-mode fibers—which result in different network-sharing strategies. We start by comparing three switching architectures considering the evolution of traffic over time: (1) full-spectrum spatial switching (full-spectrum SS); (2) wavelength switching (WS) of uncoupled spatial superchannels; and (3) independent switching (IS) of spatial and wavelength channels. IS provides high network flexibility at the cost of complex switching nodes. On the other hand, full-spectrum SS and WS simplify network nodes but reduce flexibility by switching superchannels. Simulation results indicate that WS offers poor utilization in the long term. Full-spectrum SS, in contrast, exhibits low utilization in the short term, but outperforms IS in the long term. We also propose alternative hybrid switching strategies that start with IS and change to full-spectrum SS after a certain number of spatial channels are activated. The simulations suggest that well-designed strategies for migration from IS to full-spectrum SS delay premature activation investments while saving on switching costs.**

***Index Terms*—Optical networks; Optical switching; Space-division multiplexing.**

I. Introduction

Since the invention of the Internet, information traffic has been growing exponentially, necessitating also an exponential growth in the capacity of the optical networks that support it. However, only an exponential growth in system capacity is not enough, as technological advances should also aim to minimize the networking costs. Until recently, optical communication networks have been able to provide a sustainable model of scalability using wavelength-division multiplexing (WDM) technology. For many years, it has been possible to employ WDM in optical networks with exponentially increasing capacity using only a few wavelengths. However, once the capacity of the first wavelength is exhausted, the exponential growth of demand would require an exponential increase in the number of wavelengths. In the same way, once the capacity of a fiber is exhausted, the number of fibers needs to be increased exponentially to meet the demand for traffic. In this scenario, the scalability and integration opportunities provided by space-division multiplexing (SDM) become lucrative to minimize the increase in the networking cost. SDM can be implemented with single-mode fiber bundles, multicore fibers, or multimode fibers. At first, single-mode fiber bundles can be used to take advantage of legacy infrastructure. Subsequently, as the capacity of these systems is exhausted and new deployments become necessary, solutions based on multicore fibers or multimode fibers are more appealing for adoption [1–4].

The optical networks based on the WDM technology evolved to switch lightpaths defined by their wavelength. As the capacity of a fiber has been much higher than the demand between source–destination pairs, several lightpaths originating from different source–destination pairs are usually allocated at different wavelengths to share available fiber capacity. This sharing is enabled by wavelength-selective switches (WSSs), which are able to perform wavelength switching (WS) with a high degree of flexibility. However, the clash constraint, i.e., that different lightpaths sharing the same fiber must have different wavelengths [5], also limits the utilization of the network. As the amount of information between different nodes in the network increases, so does the number of fibers needed to support that traffic. In this scenario, new forms of network-sharing approaches need to be investigated. Indeed, fiber sharing by lightpaths originating from different source–destination pairs may eventually become highly inefficient.

This paper studies switching solutions for scaling SDM networks in uncoupled spatial superchannels, such as networks with multicore fibers or bundles of single-mode

Manuscript received June 21, 2018; revised August 27, 2018; accepted October 1, 2018; published November 6, 2018 (Doc. ID 335777).

A. C. Jatoba-Neto (e-mail: alaelson@decom.fee.unicamp.br), D. A. A. Mello, and C. E. Rothenberg are with the School of Electrical and Computer Engineering, University of Campinas, Campinas, Brazil.

A. C. Jatoba-Neto is with the Federal Institute of Alagoas, Arapiraca, Brazil.

S. Ö. Arik is with Baidu Silicon Valley AI Lab, 1195 Bordeaux Dr, Sunnyvale, California 94089, USA.

J. M. Kahn is with E. L. Ginzton Laboratory, Department of Electrical Engineering, Stanford University, Stanford, California 94305, USA.

https://doi.org/10.1364/JOCN.10.000991

fibers. Networks containing fiber links with coupled spatial channels, such as multimode fibers and coupled-core multicore fibers, which require multiple-input–multiple-output (MIMO) processing to separate signals multiplexed in multiple spatial channels, are not addressed in the scope of the paper. Current optical systems use independent switching (IS), so that any wavelength channel coming from any input direction of the optical node can be routed to any output direction. Implementing IS for SDM networks with uncoupled cores would require a linear increase in the amount of WSSs used for switching, resulting in prohibitively high networking costs. Alternatively, two other architectures investigated recently have the potential to reduce the complexity of SDM switching based on high-capacity superchannels. The first approach is the WS of spatial superchannels [6–8], in which nodes are capable of simultaneously switching all the spatial channels at a specific wavelength, from any input direction to any output direction. This approach uses a smaller number of switching elements compared with IS. WS is analogous to IS implemented in only one fiber, but with wavelengths whose capacities are multiplied by the number of spatial channels available. Thus, WS is still subject to capacity losses due to the clash constraint. The second approach is full-spectrum spatial switching (full-spectrum SS), in which exclusive fibers or cores are allocated to interconnect all source–destination pairs of the network. In full-spectrum SS, there is no capacity sharing by lightpaths originating from different source–destination pairs, eliminating capacity losses because of the clash constraint. In this architecture, wavelength-selective components are not needed at pass-through network nodes, and information switching is performed with simple optical cross-connects (OXCs) [9]. Finally, the absence of interfering wavelengths from multiple source–destination pairs increases the robustness of the network and allows a possible full-spectrum nonlinear compensation [10]. As a disadvantage, low-load source–destination pairs may yield low network utilization.

Several spectral and spatial switching strategies have been studied to scale SDM networks. In Ref. [11], Khodashenas *et al.* presented various spatial and spectral allocation schemes, including WS, without addressing full-spectrum SS. Similarly, in Refs. [12,13], Siracusa *et al.* investigated resource allocation algorithms for SDM, but did not consider full-spectrum SS. In Refs. [9,14], Marom *et al.* presented a comprehensive review of node architectures for SDM switching. Node architectures with full-spectrum SS were presented, but traffic dynamicity issues were not analyzed. A similar approach was followed by Klonidis *et al.* in Ref. [2]. In Ref. [1], Arik *et al.* investigated the consequences of spatial and spectral aggregation. The work derived analytical formulas for the required number of components and the routing power to analyze the scalability of SDM networks. In Refs. [15–18], Shariati *et al.* presented several switching strategies for SDM networks, but yet did not investigate full-spectrum SS. In Ref. [19], Rottondi *et al.* presented spatially and spectrally flexible SDM architectures focused on WS. In Ref. [20], Muhammad *et al.* employed the architecture on demand concept in SDM, without considering the full-spectrum SS and WS of spatial superchannels. In Ref. [21], Muhammad *et al.* investigated the concept of filterless networks applied to SDM. An experimental demonstration of the transmission performance of connections routed in heterogeneous MCFs based on filterless node architectures has been presented by Saridis *et al.* in Ref. [22]. In Ref. [23], Fiorani *et al.* investigated the performance of SDM in data centers for different switching architectures. The paper considered full-spectrum SS, but only for a specific number of spatial channels. In Ref. [24], Hua *et al.* compared SDM and WDM networks in terms of capital expenditures (CAPEX), but the time evolution of the results was not analyzed. In Ref. [25], Jinno and Mori proposed the architecture of an integrated SDM–WSS based on a planar lightwave circuit, and Moreno-Muro *et al.* evaluated reconfigurable add-drop multiplexers (ROADMs) for flex-grid/MCF networks in Ref. [26]; however, neither study evaluated the full-spectrum SS scheme. In Refs. [27,28], Rumipamba-Zambrano *et al.* assessed the impact of space conversion on the performance of flex-grid/SDM networks, also without considering full-spectrum SS.

In Ref. [29], we evaluated network utilization as a function of the temporal evolution of traffic, for the full-spectrum SS and WS of spatial superchannels. It was observed that WS is advantageous for low requirements for the activation of spatial channels in the short term, but yields poor utilization as the traffic evolves. On the other hand, full-spectrum SS requires activation of many spatial channels in the early years, but offers high utilization in the long term, postponing new investments in the network. In this paper, we extend the results of Ref. [29] in four central facets:

- we include IS to the analysis, with the motivation of high switching flexibility;
- we propose hybrid switching strategies, which begin in the early years with IS and switch to full-spectrum SS after a certain number of spatial channels are activated. This strategy attempts to postpone the activation of new spatial channels (fibers or cores) using IS, while preserving the long-term utilization provided by full-spectrum SS;
- we evaluate the IS, full-spectrum SS, and hybrid schemes with connections of multiple rates;
- we review existing candidate nodal architectures for the actual implementation of the IS, WS, and full-spectrum SS switching schemes, and propose combining the IS and full-spectrum SS node architectures to implement hybrid switching schemes.

II. Switching Techniques

A. Node Architectures

In optical SDM networks, the signals transmitted over an optical cable have spatial and spectral degrees of freedom, as indicated in Fig. 1(a). Each optical signal can be associated with a wavelength channel λ_n ($n \in \{1, 2, \ldots, N\}$) and a spatial channel SC_m ($m \in \{1, 2, \ldots, M\}$). In this paper,

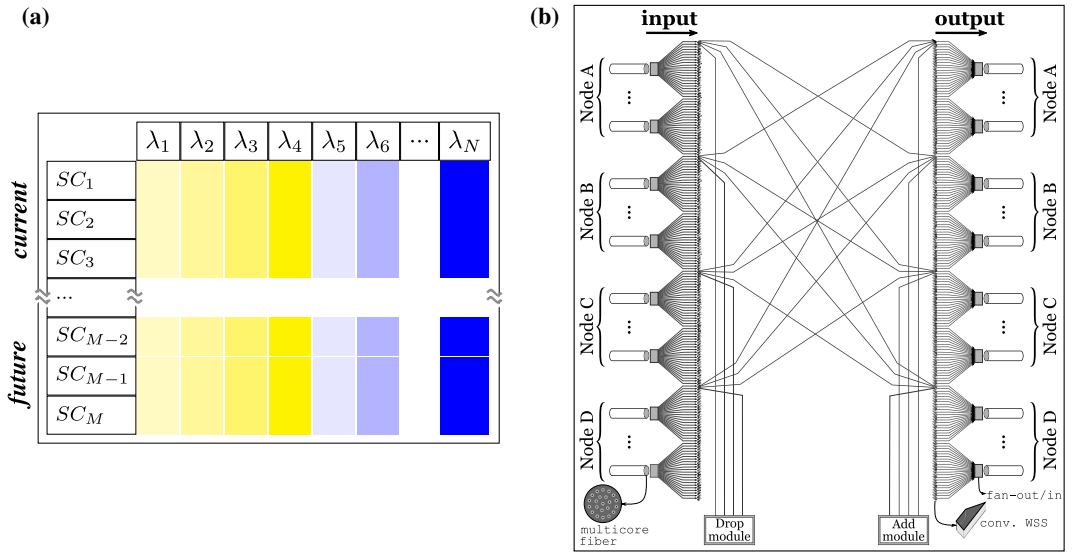

Fig. 1. IS architecture [9,14]. (a) Optical cable occupation. In the figure, SC_m denotes spatial channel m and λ_n denotes wavelength channel n. In IS, each signal using a particular wavelength channel and spatial channel can be routed independently from an input direction to an output direction. (b) Route-and-select ROADM architecture for a bundle of MCFs. For bundles of SMFs, the same structure can be used, except for the core fan-out/in, which is no longer necessary.

we assume the use of uncoupled spatial channels, such as those presented in multicore fibers or in single-mode fiber bundles.

In IS, each optical signal can be routed independently from an input direction to an output direction of the optical node. Although current networks operate with a large number of wavelength channels and a small number of spatial channels, these numbers may become more balanced as the traffic supported by the network evolves. A possible node architecture for this switching scheme is shown in Fig. 1(b), for a node degree of $L = 4$. For each input direction (node A, B, C, or D), first a spatial de-multiplexer separates the constituent spatial channels. In the case of bundles of single-mode fibers, this de-multiplexer is simply a fan-out of fibers in a cable. In the case of multicore fibers, each fiber has its own additional fan-out to separate the cores. Assuming a route-and-select architecture, there is an input/output WSS for each spatial channel SC_m (fiber or core). Each of these $2ML$ WSSs has L output/input ports, $L-1$ connected to the output/input directions, and an additional port for channel dropping/adding. Note that this configuration does not allow spatial conversion, a feature called "lane change" in Ref. [14]. In this configuration, the number of WSSs grows linearly with the number of spatial channels.

WS routes spatial superchannels, defined as a set of multiplexed spatial channels that are transmitted, received, routed, and switched as a unit. Figure 2(a) depicts the occupation of an optical cable conveying spatial superchannels. A spatial superchannel may have a variable bandwidth in the context of elastic optical networks, and may be generated by a single carrier or multiple subcarriers. Even with uncoupled spatial channels, it is advantageous to switch all spatial channels as a unit to decrease the complexity of the switching hardware [6,8]. Figure 2(b) shows a possible node architecture to perform WS. The fibers coming from an input direction are first separated. In the case of multicore fibers, a fan-out stage is required to separate the cores. Then, these signals are forwarded to a special WSS that can route all spatial channels of an input direction toward one of the $L-1$ output directions. Devices of this type are also used to aggregate distinct wavelengths in the output spatial channel. Although Fig. 2(b) shows one SDM WSS per fiber at the output and input, large-port-count devices can also be used for multiple fibers.

Full-spectrum SS, in contrast, routes spectral superchannels composed of all wavelength channels within a fiber or a core, as depicted in Fig. 3(a). The node architecture for full-spectrum SS is shown in Fig. 3(b). As for previous architectures, spectral superchannels are first separated by a cable fan-out, or a core fan-out in the case of MCFs. Then, each signal is sent to an OXC, which can be a single unit or built by multiple devices. The OXC configuration depicted in Fig. 3(b) is composed of one switching matrix per spatial channel and, therefore, does not allow spatial conversion. Note that the add/drop capability of the node depends on the number of input and output ports of the optical switching matrices. A non-blocking add/drop configuration would require $M2L \times 2L$ switching matrices. If the OXC is implemented as a single unit, then it is even possible to perform spatial conversion and improve the system capacity.

There are several possible architectures for the implementation of add/drop modules for the IS and WS schemes, such as those proposed in Ref. [30]. However, this paper focuses on the long-term deployment of full-spectrum SS, for which add/drop modules consist of a single or multiple WSSs per fiber or core to multiplex/de-multiplex the corresponding transmitted/received signals. Therefore, we do not delve into the details of add/drop modules, rather

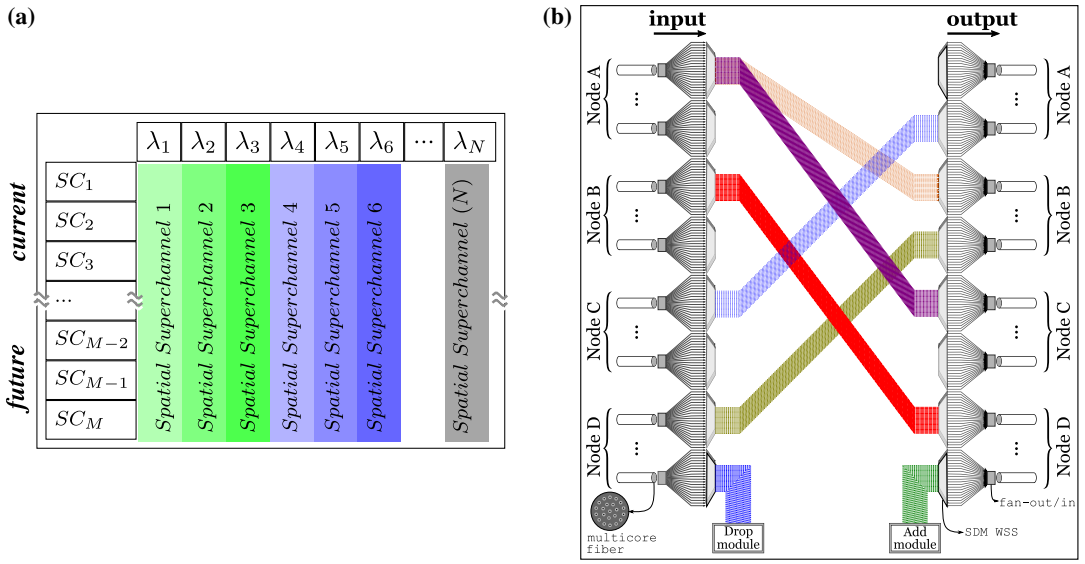

Fig. 2. WS architecture [9,14]. (a) Optical cable occupation. In the figure, SC_m denotes spatial channel m and λ_n denotes wavelength channel n. In WS, each spatial superchannel can be routed from an input direction to an output direction. (b) WS ROADM architecture for bundles of MCFs. For certain node architectures supporting MCFs and for bundles of SMFs, the core fan-out/in may no longer be necessary.

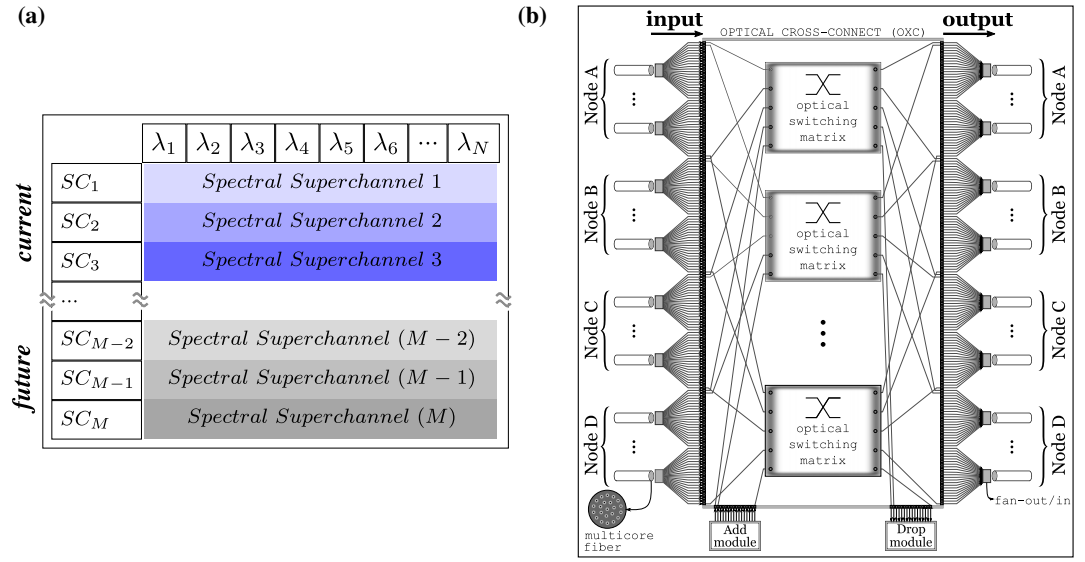

Fig. 3. Full-spectrum SS architecture [9,14]. (a) Optical cable occupation. In the figure, SC_m denotes spatial channel m and λ_n denotes wavelength channel n. In full-spectrum SS, each spectral superchannel can be routed from an input direction to an output direction. (b) Full-spectrum SS ROADM architecture for bundles of MCFs. For bundles of SMFs, the same structure can be used, except for the core fan-out/in, which is no longer necessary. The OXC may be composed of a single switching matrix or multiples matrices. The configuration depicted in the figure is composed of one switching matrix per spatial channel, and, therefore, does not allow spatial conversion. Note that the add/drop capability of the node depends on the number of input and output ports of the optical switching matrices.

explore the networking performance of the investigated solutions.

In this paper, we also evaluate hybrid switching strategies, in which the network starts deploying IS but, after the activation of M_{SC} spatial channels, full-spectrum SS is implemented to support the remaining traffic demand. This scheme segregates the network in two independent layers that are deployed in different points in time. As an example, Fig. 4 shows the evolution of the elements of a network node using the hybrid switching scheme with $M_{\mathrm{SC}} = 2$. In a scalable architecture, the node starts with $2L$ WSSs to interconnect a single spatial channel (first column). When the second spatial channel is activated, a second block of $2L$ WSSs is installed (second column). After

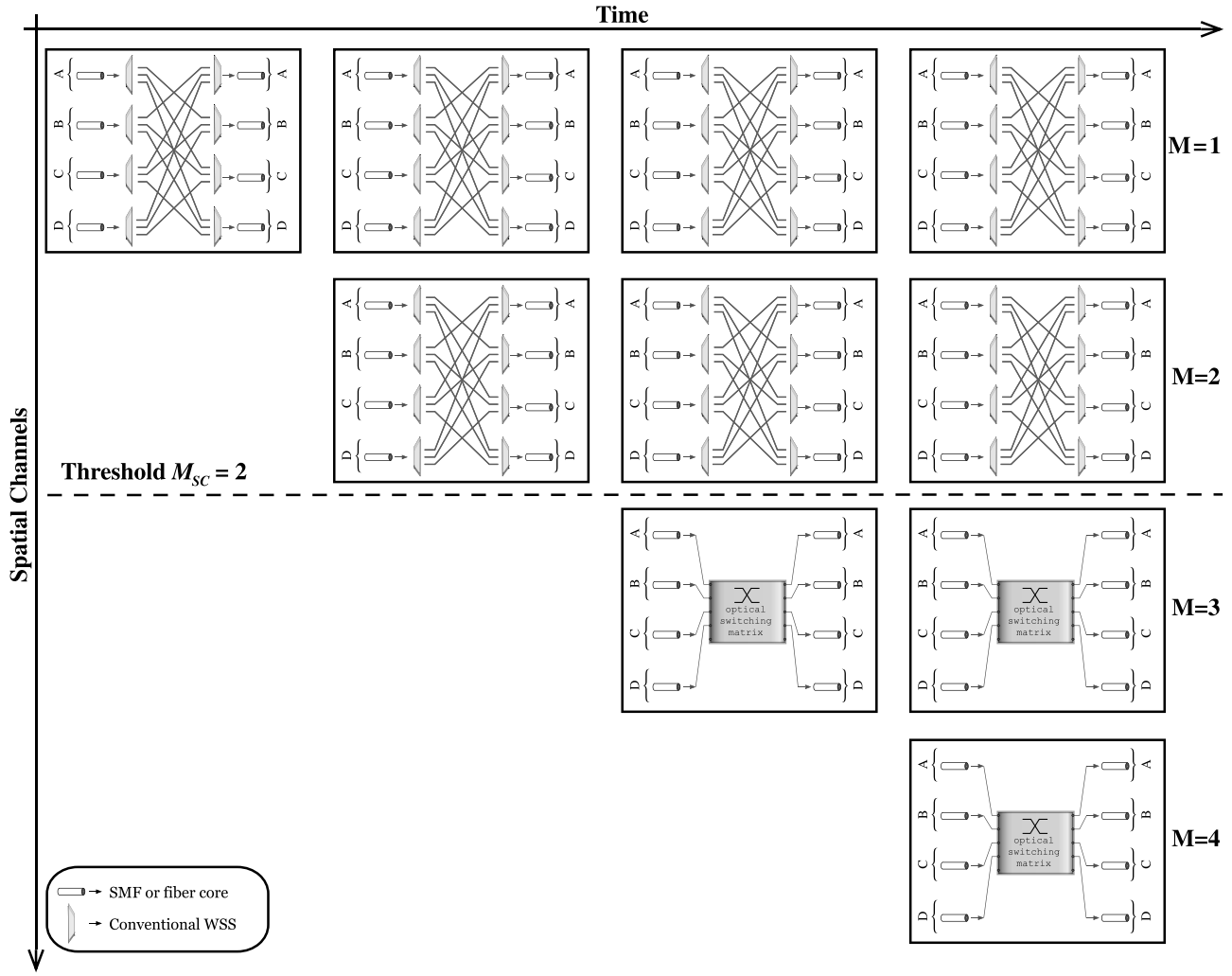

Fig. 4. Time evolution of a node that scales to support up to four spatial channels using the hybrid switching scheme with $M_{SC} = 2$. The vertical direction indicates the installed switching elements, whereas the horizontal direction represents the evolution over time. Note that the WSSs installed to support IS in the first years remain operating after switching to full-spectrum SS. The add/drop details have been omitted for clarity.

this point, the node scales by the installation of a single optical switching matrix per new spatial channel (third and fourth columns). Note that the WSSs installed to support IS in the first years remain operating.

B. Dynamic Allocation

In order to evaluate the switching techniques investigated in this paper, the corresponding dynamic allocation techniques must be defined. We classify superchannels into two classes, namely, "available" and "allocated". An available superchannel is ready to receive traffic, but all of its constituent channels are unused. It becomes an allocated superchannel if one of its constituent channels is used to accept an incoming traffic demand.

The dynamic allocation algorithm for the WS of spatial superchannels is shown in Fig. 5(a). First, the algorithm checks if there is an allocated spatial superchannel with available capacity connecting the desired source–destination pair of the request. If there is, then the request is accepted using the available capacity. Otherwise, the algorithm attempts to find an available spatial superchannel using the K shortest path algorithm. If it succeeds, this available spatial superchannel becomes allocated and the request is accepted. Otherwise, a new spatial channel is activated at all network links and the algorithm is restarted. Adding a new spatial channel creates new capacity at all existing spatial superchannels, enabling the acceptance of the incoming demand using an existing spatial superchannel with the same source–destination pair. Note that, in WS, the spectrum allocation in the first spatial channel is replicated to all other spatial channels. Although there is a small probability that a given source–destination pair is not interconnected in the first spatial channel, in the simulated traffic realizations, there is at least one spatial superchannel interconnecting a given source–destination pair, guaranteeing full connectivity.

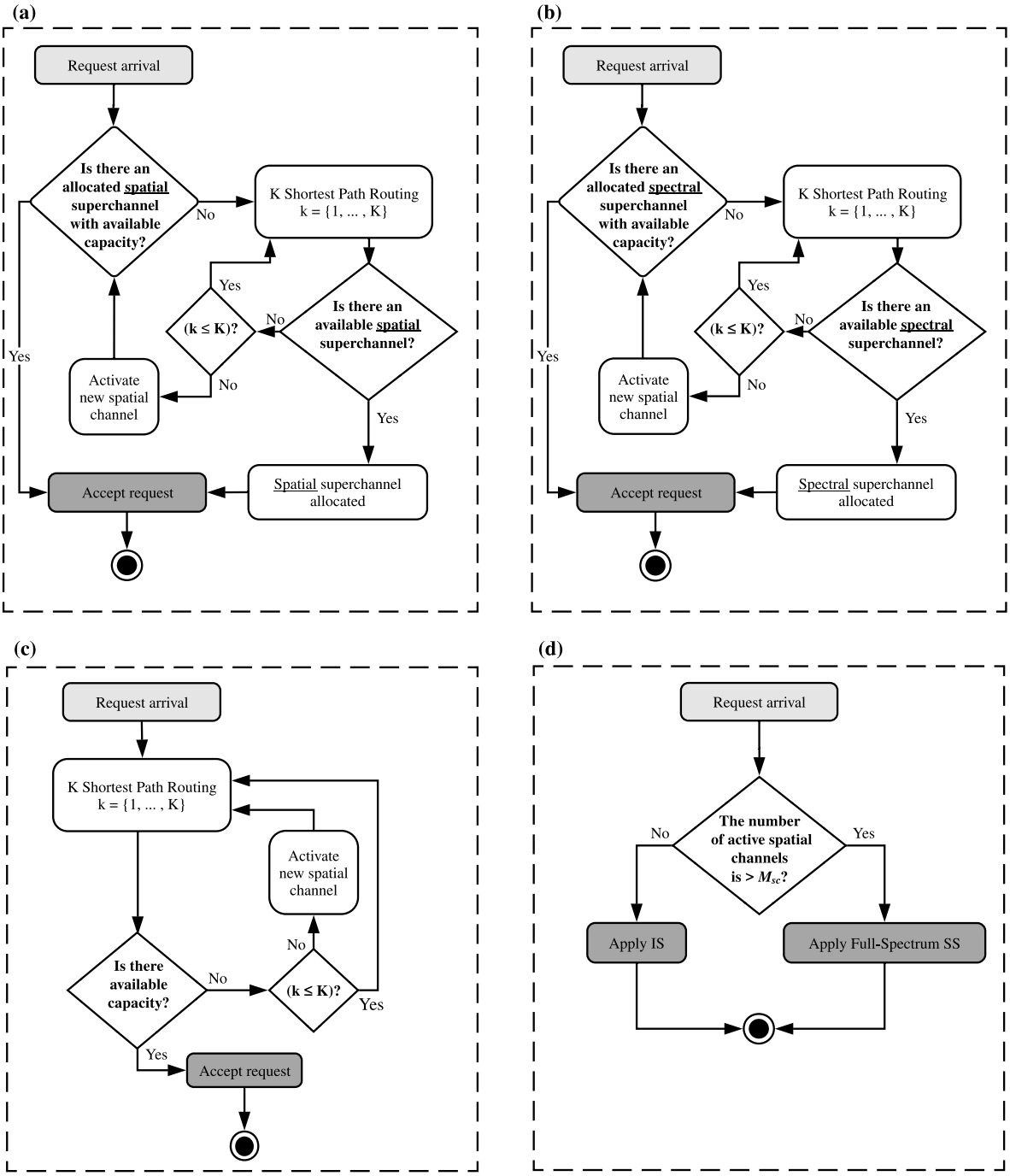

Fig. 5. Resource allocation algorithms: (a) WS, (b) full-spectrum SS, (c) IS, and (d) hybrid switching from IS to full-spectrum SS.

Analogously, full-spectrum SS allocates dynamically spectral superchannels, as depicted in Fig. 5(b). The algorithm starts by checking if there is an allocated spectral superchannel (e.g., the bandwidth of a fiber or a core) with available capacity connecting the desired source–destination pair. If there is, then the request is accepted using the available capacity. Otherwise, the algorithm attempts to find an available spectral superchannel using the K shortest path algorithm. If the search succeeds, this available spectral superchannel becomes allocated and the request is accepted. Otherwise, a new spatial channel is activated at all network links and the algorithm is restarted.

The resource allocation algorithm for IS is presented in Fig. 5(c). First, the algorithm performs conventional K shortest path routing and wavelength assignment using the first fit algorithm. If there is available capacity, then the connection is accepted. Otherwise, a new spatial channel is activated at all network links and the algorithm restarts to accept the incoming request.

The hybrid IS/full-spectrum SS scheme is depicted in Fig. 5(d). The algorithm applies IS until the first M_{SC} spatial channels are activated, then it applies full-spectrum SS for the remaining time. The idea behind hybrid switching is that IS should provide sufficiently fine granularity for switching connections using a low number of active spatial channels. However, full-spectrum SS should be used if the number of active spatial channels

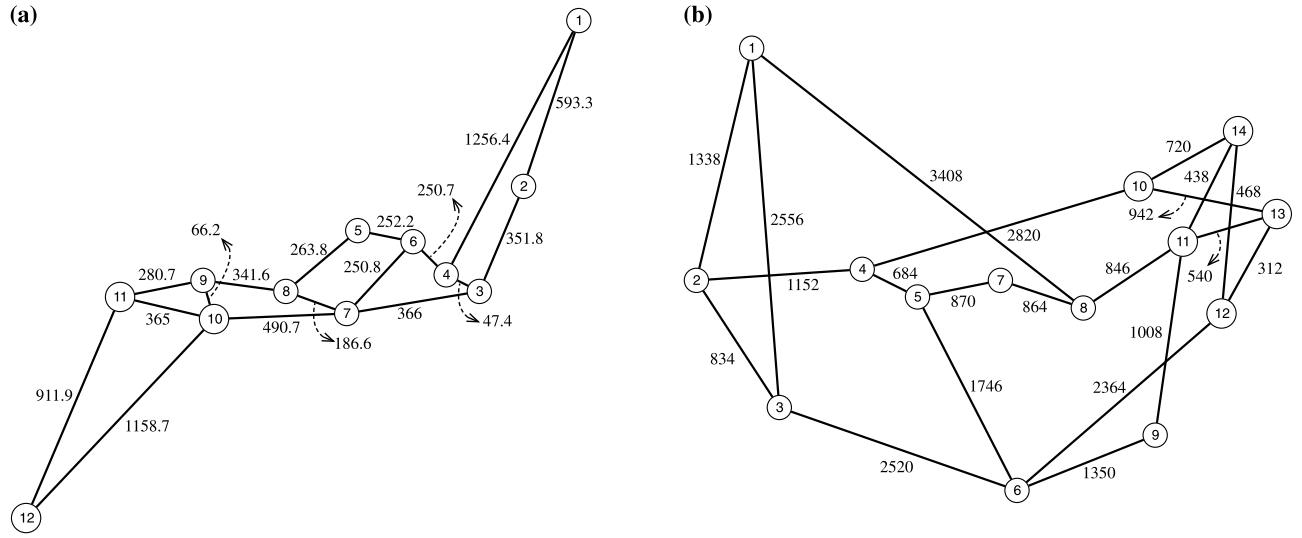

Fig. 6. Simulated network topologies: (a) JPN12. (b) NSFNET. In the figure, distances are expressed in kilometers.

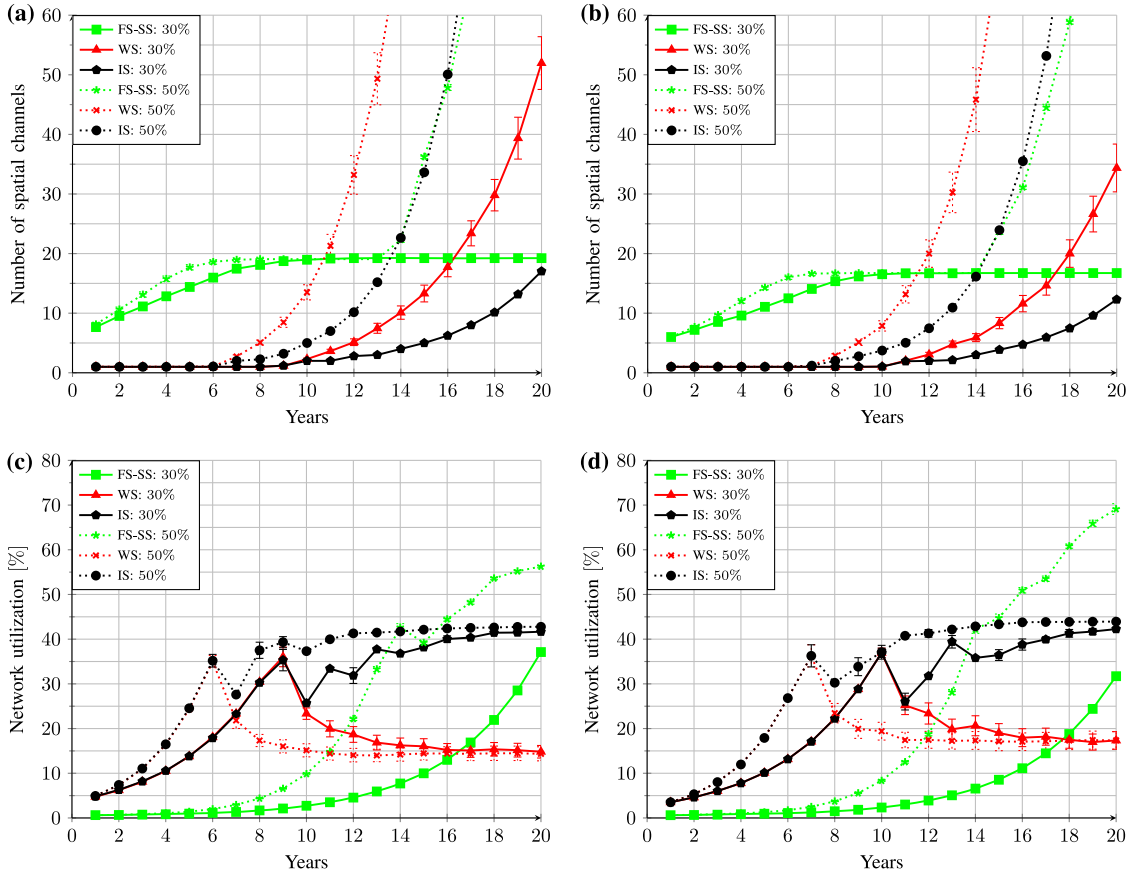

Fig. 7. Number of spatial channels (top) and network utilization (bottom) for the JPN12 (left) and NSFNET (right) networks. The CAGR is set to 30% and 50%. In the figure, FS-SS stands for full-spectrum SS.

is high enough to avoid the clash constraint and simplify the switching nodes. In this way, the investments associated with the activation of new spatial channels (e.g., with inline amplifiers) would be delayed.

We do not consider the reallocation of existing traffic in any of the resource allocation schemes investigated, as it leads to frequent service disconnections and eventual network transients. In particular, this would be highly undesirable in heavily loaded networks with multiple activated spatial channels, as in the case of our study.

III. Simulation of Time Evolution

A. Simulation Setup

We evaluate the investigated switching strategies using a discrete-event simulator with incremental traffic, i.e., accepted connections are never torn down. The simulation setup is the same as in Ref. [29], with the inclusion of the IS and hybrid IS/full-spectrum SS strategies. We simulate an optical bandwidth of 4.8 THz (as 96×50 GHz frequency slots). Demands of capacity $R \times 100$ Gb/s ($R \in \{1, 4, 10\}$) are allocated over $R \times 50$ GHz slots. We assume a constant spectral efficiency for demands of multiple rates to allow an equivalent comparison among the different rate granularities. Routing is performed using Yen's K shortest path algorithm with $K = 3$ [31]. Wavelength assignment follows the first-fit policy. A 3 Tb/s network traffic in the first year is increased annually following compound annual growth rates (CAGRs) of 30% or 50%. These settings agree with the Cisco Visual Networking Index [32], which predicts CAGRs from 20% to 50% depending on the geographic region. Thus, for demands of $R \times 100$ Gb/s at constant R, the traffic $T(i)$ allocated in the year $i = 1, 2, 3, \ldots$ is given by

$$T(i) = \left\lceil \frac{30}{R} \times (1 + \text{CAGR})^{i-1} \right\rceil \times R \times 100 \text{ Gb/s}, \quad (1)$$

where $\lceil x \rceil$ is the smallest integer greater than or equal to x. In simulations with mixed values of $R \in \{1, 4, 10\}$, R is set to 1 in Eq. (1). In addition, if the last generated demand yields an accumulated traffic higher than $T(i)$, then this demand is discarded, and a new demand is generated until the total traffic matches $T(i)$ exactly.

Two network topologies are simulated (Fig. 6): (i) the National Science Foundation Network (NSFNET) [33], with 14 nodes and 21 bidirectional links, and (ii) the Japan Photonic Network (JPN12) [34], with 12 nodes

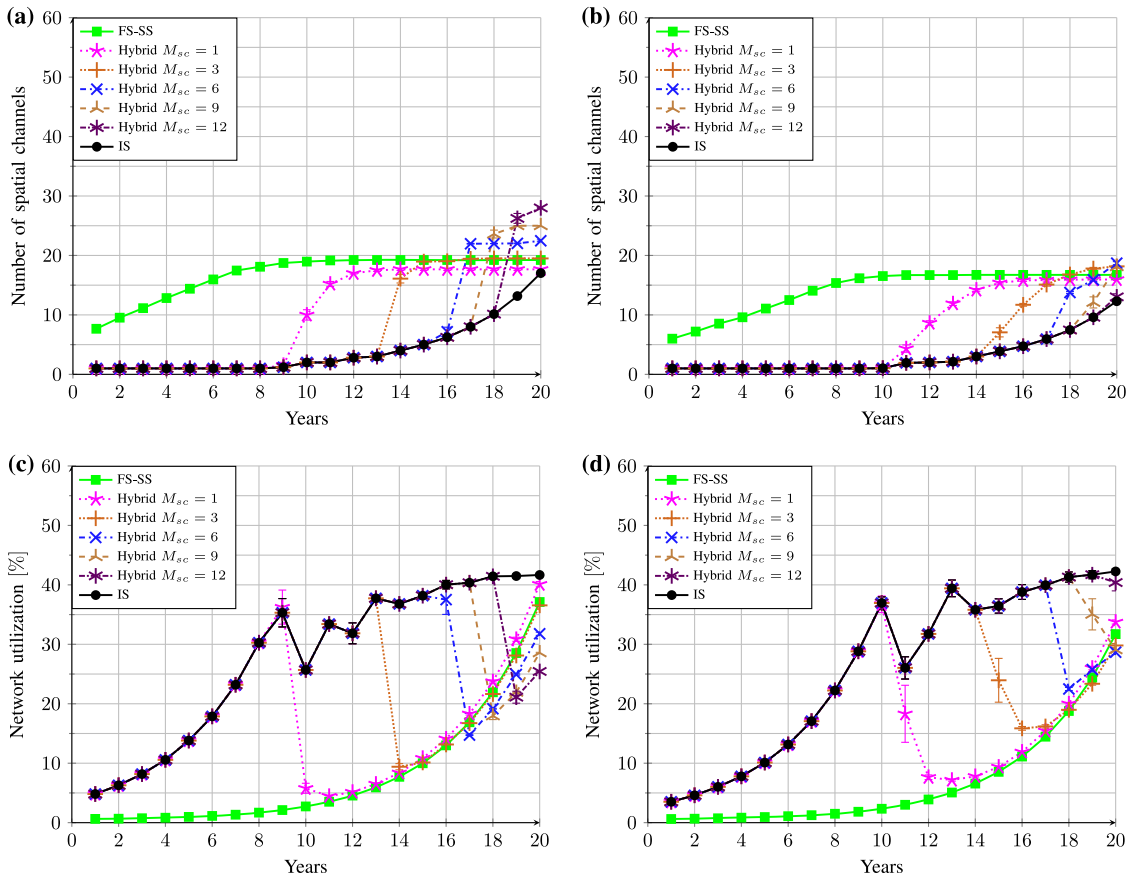

Fig. 8. Number of active spatial channels (top) and network utilization (bottom) for the JPN12 (left) and NSFNET (right) networks, at a CAGR of 30%. In the figure, FS-SS stands for full-spectrum SS.

and 17 bidirectional links. The simulation is non-blocking, as a new spatial channel is added to all network links whenever the network capacity is not enough to accommodate an incoming request. This is a simulation resource used to maintain consistency among the architectures of all network nodes. Indeed, under heavy traffic, several spatial channels are activated every year and, under these conditions, activating spatial channels only in overloaded links would lead to little change in the overall results. We assume a uniform distribution between all source–destination pairs. Space and wavelength conversion are not supported. The network performance is assessed by the annual change in two metrics: the total number of active spatial channels and the amount of network utilization, U, which is defined as

$$U = \frac{\sum_{i=1}^{n_r} E_i \cdot N_i}{N \cdot M \cdot E_g}, \tag{2}$$

where n_r is the number of generated demands, E_i is the hop-count traversed by the demand i, N_i is the number of frequency slots used by the demand i, N is the number of frequency slots supported by spatial channels, M is the number of active spatial channels, and E_g is the number of edges in the network graph. Each simulation was calculated as the average of 30 runs. Confidence intervals are computed using a 95% confidence level.

B. Pure Switching Strategies

Figure 7 shows the number of active spatial channels and the network utilization metrics for the JPN12 and NSFNET networks. The simulations consider only 100 Gb/s demands [$R = 1$ in Eq. (1)]. The curves are the same as in Ref. [29], with the inclusion of IS. The simulation results reveal similar trends for the two topologies. For the JPN12 network, WS and IS require just one spatial channel until years 6 and 9, for CAGRs of 50% and 30%, respectively. The same behavior can be observed for the NSFNET network, which indicates that IS and WS require lower investments at low network loads. The network utilizations of WS and IS exhibit the best performance in the first years, achieving a maximum of 35% each. After that, the utilization for WS drops, and remains constant below 20%. The peak coincides with the exhaustion of capacity of the first spatial channel, after which a second spatial channel is activated, decreasing utilization. After this, the number of spatial channels also grows exponentially, and the low network utilization remains. Therefore, although this spectral efficiency could grow with better wavelength assignment schemes, WS might not be an attractive solution for the long term. The flexibility provided by IS enables better long-term utilization performance, achieving values above 40%. Full-spectrum SS, on the other hand, requires

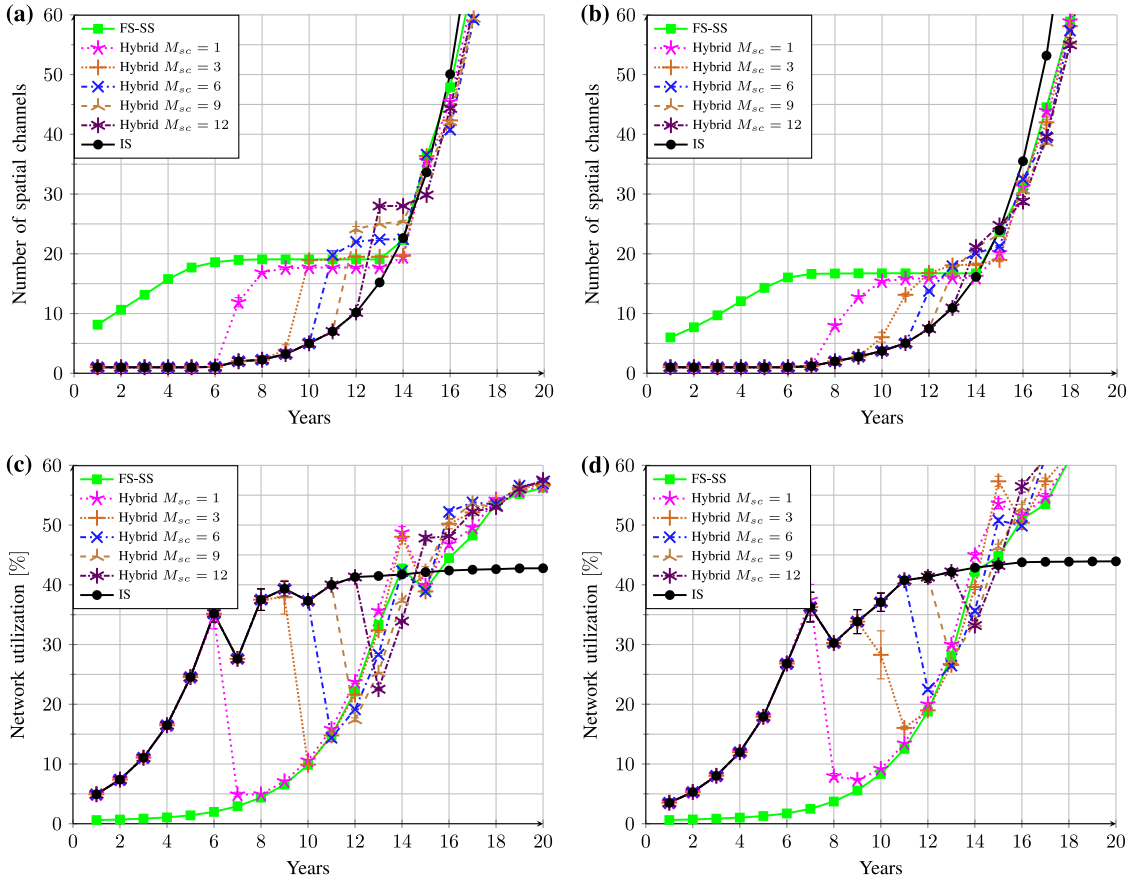

Fig. 9. Number of active spatial channels (top) and network utilization (bottom) for the JPN12 (left) and NSFNET (right) networks, at a CAGR of 50%. In the figure, FS-SS stands for full-spectrum SS.

the activation of a large number of a spatial channels in the first years, until all source–destination pairs are interconnected by a separate fiber. Before this point is reached, the utilization remains at very low values. However, in the long term, although providing a lower switching flexibility, full-spectrum SS outperforms IS in terms of utilization, as there are no capacity losses due to the clash constraint. This can be observed for a CAGR of 50%, for which the utilization of full-spectrum SS reaches around 55% for the JPN12 network and 70% for the NSFNET.

C. Hybrid Switching Strategies

On the one hand, IS requires a low number of spatial channels at the cost of a high switching complexity. On the other hand, full-spectrum SS provides high long-term utilization and greatly simplifies switching nodes, but requires the activation of a large number of spatial channels in the first years. Hybrid strategies attempt to combine the best of these two options. We have evaluated the performance of hybrid switching strategies starting from IS and migrating to full-spectrum SS after the activation of $M_{SC} \in \{1, 3, 6, 9, 12\}$ spatial channels. The simulations consider 100 Gb/s demands. Figure 8 shows the evolution of the number of spatial channels and network utilization for a CAGR of 30% for the JPN12 and NSFNET networks. Clearly, hybrid switching with $M_{SC} = 1$ delays the activation of a high number of spatial channels by 9–10 years while preserving a low node complexity. It even reduces the number of active spatial channels in the long term, compared with full-spectrum SS, by providing a network layer with one dimension and wavelength granularity. It is interesting to observe that a late implementation of hybrid switching increases the number of active dimensions in year 20 because of a lower utilization factor. This higher utilization provided by full-spectrum SS at heavy traffic becomes more evident in Fig. 9 for a CAGR of 50%. In year 20, all hybrid strategies reach an equivalent network utilization, which is considerably higher than that for IS. However, as observed in Fig. 8 for a CAGR of 30%, a late implementation of full-spectrum SS creates an intermediate regime where the number of active spatial channels for the hybrid strategies is higher than that for full-spectrum SS. These results suggest that the implementation of hybrid strategies with M_{SC} equal to 1–3 may provide a good compromise between activation and switching costs.

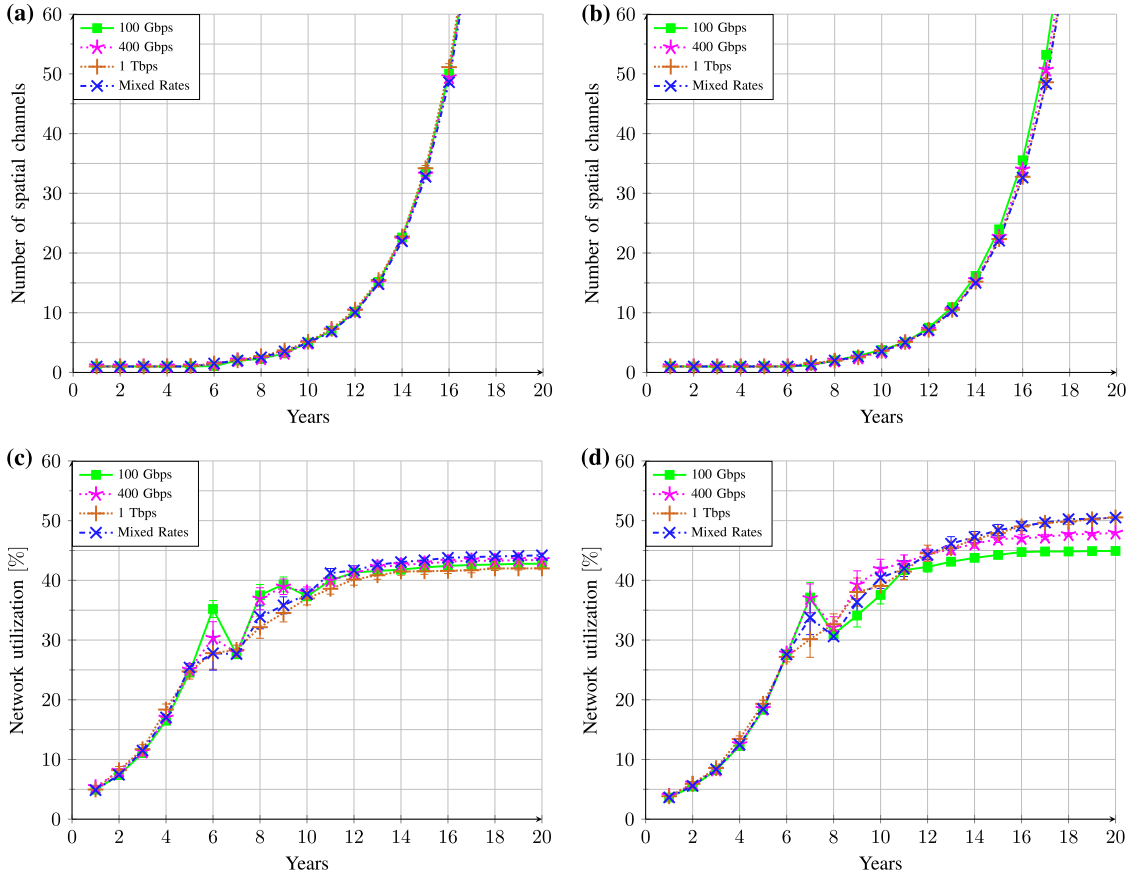

Fig. 10. IS of demands with multiple rates. Number of active spatial channels (top) and network utilization (bottom) for the JPN12 (left) and NSFNET (right) networks, at a CAGR of 50%, are shown. The "mixed rates" curves correspond to a set of demands distributed uniformly among 100 Gb/s, 400 Gb/s, and 1 Tb/s.

D. Multiple Rates

We also evaluated the sensitivity of the IS, full-spectrum SS, and hybrid ($M_{SC} = 3$) schemes under connections with multiple rates. We simulate demands of 100 Gb/s, 400 Gb/s, and 1 Tb/s using bandwidths of, respectively, 50, 200, and 500 GHz, assuming a CAGR of 50%. We assume a constant spectral efficiency for multiple rate demands to allow an equivalent comparison among the multiple configurations. The evaluation of channels with multiple spectral efficiencies would lead to further displacements in the evaluated curves, which, however, would also be small due to the high simulated growth rates. There are two main phenomena that affect the network performance when working with demands for higher rates and bandwidths. First, for a given annual traffic in bit/s, the number of demands decreases. For example, although an annual traffic of 3 Tb/s generates 30×100 Gb/s demands, in the simulations with mixed rates, this could generate demands of only 3×1 Tb/s. This reduction in the number of demands helps to reduce the fragmentation of the network. On the other hand, it is easier to accommodate 100 Gb/s demands than 1 Tb/s demands using existing spectrum fragments. The advantages and disadvantages of each configuration depend on the corresponding switching scheme and network topology. Figure 10 shows the performance of IS under connections of multiple rates. While the differences in performance are negligible for the JPN12 network, for the NSFNET the simulations with 1 Tb/s and mixed rates exhibit a slight long-term advantage compared with the 100-Gb/s-only scenario. Again, this difference in performance can be explained by a more compact spectrum allocation enabled by high-bandwidth demands. The results for the full-spectrum SS scheme are shown in Fig. 11. In this case, the reduction in the number of demands is highly beneficial in the first years, as the resource allocation scheme allocates entire fibers/cores for each source–destination pair. Thus, the number of source–destination pairs to be interconnected and, consequently, the number of installed spatial channels, is strongly reduced. In the long term, there is a slight loss in performance for the configurations that contain 1 Tb/s channels, probably because the total fiber spectrum is not a multiple of 500 GHz and, therefore, the last portion of the spectrum is poorly utilized. The performance of the hybrid switching scheme with $M_{SC} = 3$ is presented in Fig. 12. In intermediate regimes, the network performance changes slightly depending on the traffic mix and the network topology. In the long term, the behavior of the curves is similar to that in the full-spectrum SS case, with a small performance penalty for configurations with 1 Tb/s

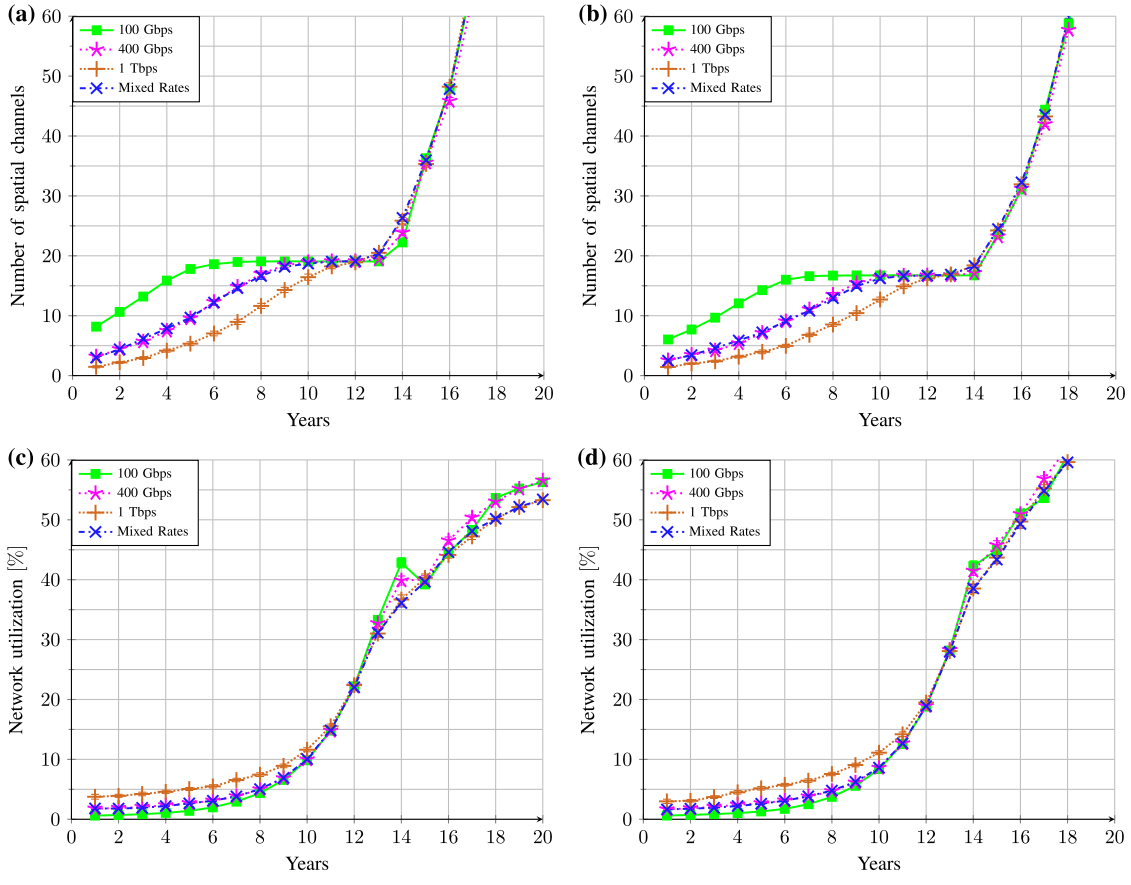

Fig. 11. Full-spectrum SS of demands with multiple rates. Number of active spatial channels (top) and network utilization (bottom) for the JPN12 (left) and NSFNET (right) networks, at a CAGR of 50%, are shown. The "mixed rates" curves correspond to a set of demands distributed uniformly among 100 Gb/s, 400 Gb/s, and 1 Tb/s.

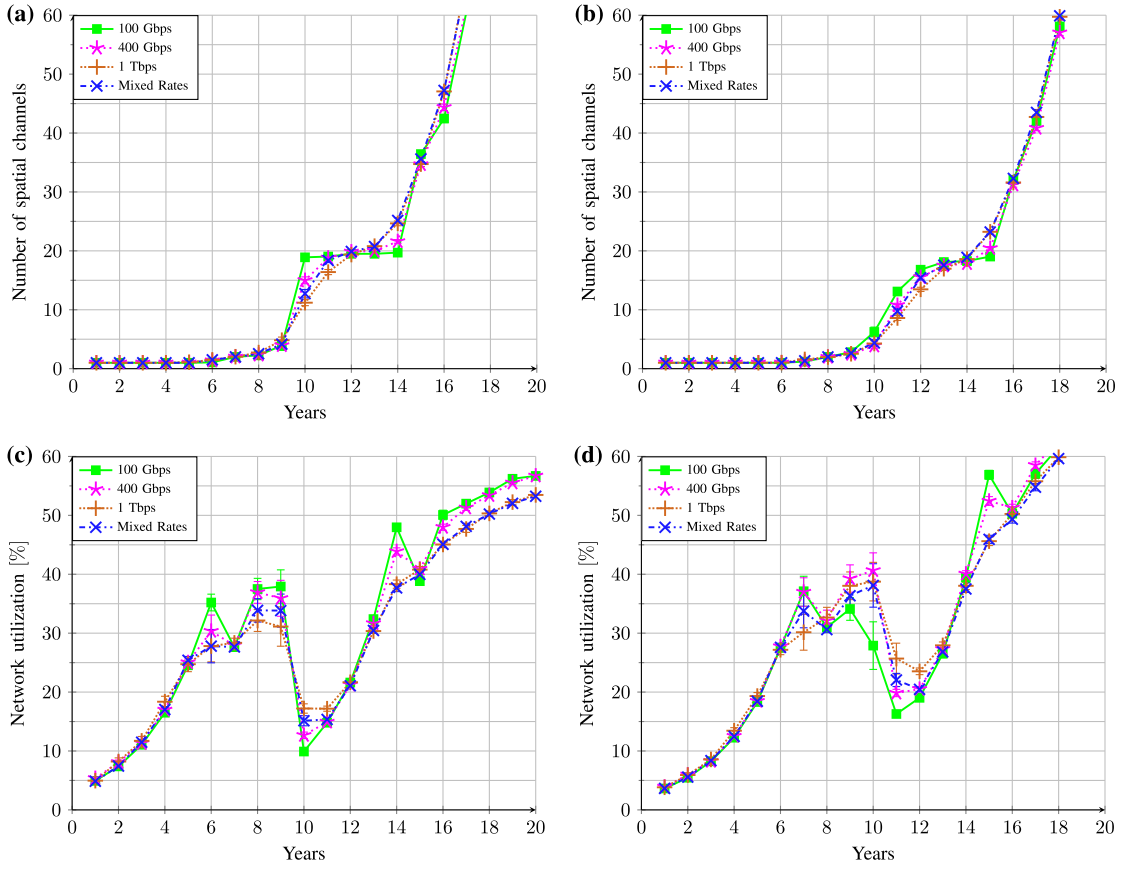

Fig. 12. Hybrid switching ($M_{SC} = 3$) of demands with multiple rates. Number of active spatial channels (top) and network utilization (bottom) for the JPN12 (left) and NSFNET (right) networks, at a CAGR of 50%, are shown. The "mixed rates" curves correspond to a set of demands distributed uniformly among 100 Gb/s, 400 Gb/s, and 1 Tb/s.

demands because of the unoccupied residual portion of the spectrum. In any case, it can be observed that the network behavior exhibits little dependence on the traffic mix, and that the long-term advantage of full-spectrum SS and the hybrid schemes compared with the IS solution is preserved.

E. Additional Considerations

The results presented in this paper refer only to network performance matters, and do not address techno-economic issues—such as the cost of money and the cost-reduction curve for network equipment over time—which are left to a future work. Clearly, the use of full-spectrum SS involves the premature activation of spatial channels, which is, however, alleviated by the hybrid schemes. Considering fibers or cores are already available in the operator's infrastructure, the activation of spatial channels involves the installation of optical amplifiers and optical switching matrices throughout the network. Although the cost of an early installation of these devices is considerable, there are three positive factors to be taken into account. First, optical switching matrices are considerably cheaper than the WSSs that would be installed in the case of IS implementation. Second, the optical switching matrices have lower insertion losses compared with WSSs, which has the potential to reduce the cost of signal regeneration. Finally, the use of full-spectrum SS reduces the long-term use of spatial channels, delaying possible investments in the installation of new fibers.

IV. Conclusion

In typical WDM networks, the available capacity in a fiber is much higher than the traffic demand between the source—destination pairs of the network. For this reason, different wavelengths are allocated to different source—destination pairs in order to share the available capacity. However, this sharing leads to capacity losses because of the clash constraint. In SDM networks, however, the capacity demand between a source—destination pair may approach that of a fiber, and new forms of infrastructure sharing are required for better efficiency. In this paper, we investigate four switching architectures, which in turn correspond to different types of network-sharing approaches. WS of spatial superchannels reveals poor long-term spectral efficiency compared with the other strategies. On the other hand, full-spectrum SS outperforms IS in terms of network utilization in the long term. This can be explained by the fact that full-spectrum SS

switching avoids spectrum fragmentation and capacity losses due to the clash constraint. As full-spectrum SS requires the activation of a large number of spatial channels in a short period of time, we investigate hybrid switching strategies combining IS in the first years with full-spectrum SS for the long term. This option is found to reduce investments in the first years while preserving the long-term spectral efficiency. In addition, simulation results indicate that changing from IS to full-spectrum SS in the first years reduces the number of installed spatial channels in intermediate regimes.

Acknowledgment

At Unicamp, this work was supported by CNPq and by the FAPESP grants 2015/04382-0 and 2015/24341-7. This is an extended version of Ref. [29].

References

[1] S. O. Arik, K.-P. Ho, and J. M. Kahn, "Optical network scaling: roles of spectral and spatial aggregation," *Opt. Express*, vol. 22, no. 24, pp. 29868–29887, Dec. 2014.

[2] D. Klonidis, F. Cugini, O. Gerstel, M. Jinno, V. López, E. Palkopoulou, M. Sekiya, D. Siracusa, G. Thouénon, and C. Betoule, "Spectrally and spatially flexible optical network planning and operations," *IEEE Commun. Mag.*, vol. 53, no. 2, pp. 69–78, Feb. 2015.

[3] P. J. Winzer, "Spatial multiplexing in fiber optics: the 10x scaling of metro/core capacities," *Bell Labs Tech. J.*, vol. 19, pp. 22–30, Sept. 2014.

[4] G. M. Saridis, D. Alexandropoulos, G. Zervas, and D. Simeonidou, "Survey and evaluation of space division multiplexing: from technologies to optical networks," *IEEE Commun. Surv. Tutorials*, vol. 17, no. 4, pp. 2136–2156, Aug. 2015.

[5] R. M. Krishnaswamy and K. N. Sivarajan, "Design of logical topologies: a linear formulation for wavelength-routed optical networks with no wavelength changers," *IEEE/ACM Trans. Netw.*, vol. 9, no. 2, pp. 186–198, Apr. 2001.

[6] N. K. Fontaine, T. Haramaty, R. Ryf, H. Chen, L. Miron, L. Pascar, M. Blau, B. Frenkel, L. Wang, Y. Messaddeq, S. LaRochelle, R.-J. Essiambre, Y.-M. Jung, Q. Kang, J. K. Sahu, S.-U. Alam, D. J. Richardson, and D. M. Marom, "Heterogeneous space-division multiplexing and joint wavelength switching demonstration," in *Optical Fiber Communications Conf. (OFC)*, Los Angeles, California, Mar. 2015, pp. 1–3.

[7] L. E. Nelson, M. D. Feuer, K. Abedin, X. Zhou, T. F. Taunay, J. M. Fini, B. Zhu, R. Isaac, R. Harel, G. Cohen, and D. M. Marom, "Spatial superchannel routing in a two-span ROADM system for space division multiplexing," *J. Lightwave Technol.*, vol. 32, no. 4, pp. 783–789, Feb. 2014.

[8] M. D. Feuer, L. E. Nelson, K. S. Abedin, X. Zhou, T. F. Taunay, J. F. Fini, B. Zhu, R. Isaac, R. Harel, G. Cohen, and D. M. Marom, "ROADM system for space division multiplexing with spatial superchannels," in *Optical Fiber Communications Conf. and The Natl. Fiber Optic Engineers Conf. (OFC/NFOEC)*, Anaheim, California, Mar. 2013, pp. 1–3.

[9] D. M. Marom, P. D. Colbourne, A. D'Errico, N. K. Fontaine, Y. Ikuma, R. Proietti, L. Zong, J. M. Rivas-Moscoso, and I. Tomkos, "Survey of photonic switching architectures and technologies in support of spatially and spectrally flexible optical networking (invited)," *J. Opt. Commun. Netw.*, vol. 9, no. 1, pp. 1–26, Jan. 2017.

[10] C. Xia, X. Liu, S. Chandrasekhar, N. K. Fontaine, L. Zhu, and G. Li, "Multi-channel nonlinearity compensation of PDM-QPSK signals in dispersion-managed transmission using dispersion-folded digital backward propagation," *Opt. Express*, vol. 22, no. 5, pp. 5859–5866, Mar. 2014.

[11] P. S. Khodashenas, J. M. Rivas-Moscoso, D. Siracusa, F. Pederzolli, B. Shariati, D. Klonidis, E. Salvadori, and I. Tomkos, "Comparison of spectral and spatial super-channel allocation schemes for SDM networks," *J. Lightwave Technol.*, vol. 34, no. 11, pp. 2710–2716, June 2016.

[12] D. Siracusa, F. Pederzolli, D. Klonidisz, V. Lopéz, and E. Salvadori, "Resource allocation policies in SDM optical networks (invited)," in *Int. Conf. Optical Network Design and Modeling (ONDM)*, Pisa, Italy, May 2015, pp. 168–173.

[13] D. Siracusa, F. Pederzolli, P. S. Khodashenas, J. M. Rivas-Moscoso, D. Klonidis, E. Salvadori, and I. Tomkos, "Spectral vs. spatial super-channel allocation in SDM networks under independent and joint switching paradigms," in *European Conf. Optical Communication (ECOC)*, Valencia, Spain, Sept. 2015, pp. 1–3.

[14] D. M. Marom and M. Blau, "Switching solutions for WDM-SDM optical networks," *IEEE Commun. Mag.*, vol. 53, no. 2, pp. 60–68, Feb. 2015.

[15] B. Shariati, P. Sayyad Khodashenas, J. M. Rivas Moscoso, S. Ben-Ezra, D. Klonidis, F. Jiménez, L. Velasco, and I. Tomkos, "Evaluation of the impact of different SDM switching strategies in a network planning scenario," in *Optical Fiber Communications Conf. (OFC)*, Anaheim, California, Mar. 2016, pp. 1–3.

[16] B. Shariati, D. Klonidis, I. Tomkos, D. Marom, M. Blau, S. Ben-Ezra, M. Gerola, D. Siracusa, J. Macdonald, N. Psaila, C. Sanchez-Costa, A. D. Ellis, J. F. Ferran, and F. Jimenez, "Realizing spectrally-spatially flexible optical networks," *IEEE Photon. Soc. News*, vol. 31, no. 6, pp. 4–9, Dec. 2017.

[17] B. Shariati, J. M. Rivas-Moscoso, D. M. Marom, S. Ben-Ezra, D. Klonidis, L. Velasco, and I. Tomkos, "Impact of spatial and spectral granularity on the performance of SDM networks based on spatial superchannel switching," *J. Lightwave Technol.*, vol. 35, no. 13, pp. 2559–2568, July 2017.

[18] B. Shariati, D. Klonidis, D. Siracusa, F. Pederzolli, J. M. Rivas-Moscoso, L. Velasco, and I. Tomkos, "Impact of traffic profile on the performance of spatial superchannel switching in SDM networks," in *European Conf. on Optical Communication (ECOC)*, Sept. 2016.

[19] C. Rottondi, P. Boffi, P. Martelli, and M. Tornatore, "Routing, modulation format, baud rate and spectrum allocation in optical metro rings with flexible grid and few-mode transmission," *J. Lightwave Technol.*, vol. 35, no. 1, pp. 61–70, Jan. 2017.

[20] A. Muhammad, G. Zervas, and R. Forchheimer, "Resource allocation for space-division multiplexing: optical white box versus optical black box networking," *J. Lightwave Technol.*, vol. 33, no. 23, pp. 4928–4941, Dec. 2015.

[21] A. Muhammad, M. Furdek, G. Zervas, and L. Wosinska, "Filterless networks based on optical white boxes and SDM," in *European Conf. Optical Communication (ECOC)*, Dusseldorf, Germany, Sept. 2016, pp. 1–3.

[22] G. M. Saridis, B. J. Puttnam, R. S. Luis, W. Klaus, T. Miyazawa, Y. Awaji, G. Zervas, D. Simeonidou, and N. Wada, "Experimental demonstration of a flexible filterless and bidirectional SDM optical metro/inter-DC network," in

European Conf. Optical Communication (ECOC), Dusseldorf, Germany, Sept. 2016, pp. 1–3.

[23] M. Fiorani, M. Tornatore, J. Chen, L. Wosinska, and B. Mukherjee, "Spatial division multiplexing for high capacity optical interconnects in modular data centers," *J. Opt. Commun. Netw.*, vol. 9, no. 2, pp. A143–A153, Feb. 2017.

[24] N. Hua, Y. Li, and X. Zheng, "Capex benefit analysis of space division multiplexing (SDM) optical networks," in *Int. Conf. Optical Communications and Networks (ICOCN)*, Nanjing, China, July 2015, pp. 1–3.

[25] M. Jinno and Y. Mori, "Unified architecture of an integrated SDM-WSS employing a PLC-based spatial beam transformer array for various types of SDM fibers," *J. Opt. Commun. Netw.*, vol. 9, no. 2, pp. A198–A206, Feb. 2017.

[26] F.-J. Moreno-Muro, R. Rumipamba-Zambrano, P. Pavón-Marino, J. Perelló, J. M. Gené, and S. Spadaro, "Evaluation of core-continuity-constrained ROADMs for flex-grid/MCF optical networks," *J. Opt. Commun. Netw.*, vol. 9, no. 11, pp. 1041–1050, Nov. 2017.

[27] R. Rumipamba-Zambrano, F.-J. Moreno-Muro, P. Pavon-Marino, J. Perello, S. Spadaro, and J. Sole-Pareta, "Assessment of flex-grid/MCF optical networks with ROADM limited core switching capability," in *Int. Conf. Optical Network Design and Modeling (ONDM)*, Budapest, Hungary, May 2017, pp. 1–6.

[28] R. Rumipamba-Zambrano, F. J. Moreno-Muro, J. Perelló, P. Pavón-Mariño, and S. Spadaro, "Space continuity constraint in dynamic flex-grid/SDM optical core networks: an evaluation with spatial and spectral super-channels," *Comput. Commun.*, vol. 126, pp. 38–49, Aug. 2018.

[29] A. C. Jatoba-Neto, C. E. Rothenberg, D. A. A. Mello, S. O. Arik, and J. M. Kahn, "Scaling optical networks using full-spectrum spatial switching," in *IEEE Int. Conf. on High Performance Switching and Routing (HPSR)*, Campinas-SP, Brazil, June 2017, pp. 1–6.

[30] J. M. Rivas-Moscoso, B. Shariati, D. M. Marom, D. Klonidis, I. Tomkos, and I. Tomkos, "Comparison of CD(C) ROADM architectures for space division multiplexed networks," in *Optical Fiber Communication Conf. (OFC)*, Washington DC, Mar. 2017, paper Th2A.45.

[31] J. Y. Yen, "Finding the K shortest loopless paths in a network," *Manage. Sci.*, vol. 17, no. 11, pp. 712–716, 1971.

[32] "Cisco Visual Networking Index: Forecast and Methodology, 2016–2021," White paper, June 2017. Available: https://www.cisco.com/c/en/us/solutions/collateral/service-provider/visual-networking-index-vni/complete-white-paper-c11-481360.pdf

[33] A. Betker, C. Gerlach, R. Hülsermann, M. Jäger, M. Barry, S. Bodamer, J. Späth, C. Gauger, and M. Köhn, "Reference transport network scenarios," MultiTeraNet Report, July 2003.

[34] "Japan photonic network model," 2013 [Online]. Available: http://www.ieice.org/cs/pn/jpn/jpnm.html.